ACS APPLIED MATERIALS & INTERFACES

Letter

www.acsami.org

A Facile Strategy toward Conjugated Polyelectrolyte with Oligopeptide as Pendants for Biological Applications

Jie Liu, Guangxue Feng, Junlong Geng, and Bin Liu*

Department of Chemical and Biomolecular Engineering, National University of Singapore, 4 Engineering Drive 4, Singapore 117576, Singapore

Supporting Information

ABSTRACT: We report a facile yet efficient strategy to synthesize biofunctionalized conjugated polyelectrolyte using click reaction between an amphiphilic oligopeptide (R10) and organic soluble polyfluorene (PF) as an example. PF-R10 shows the absorption and emission maxima at ~380 and ~430 nm in water, respectively. In addition, it exhibits enhanced fluorescence in acidic circumstance as compared to that in neutral environment because of reduced aggregation, which is confirmed by laser light scattering and atomic force microscopy studies. In view of the penetration property of the grafted R10 peptide, PF-R10 shows excellent cell uptake and labeling ability in cellular imaging.

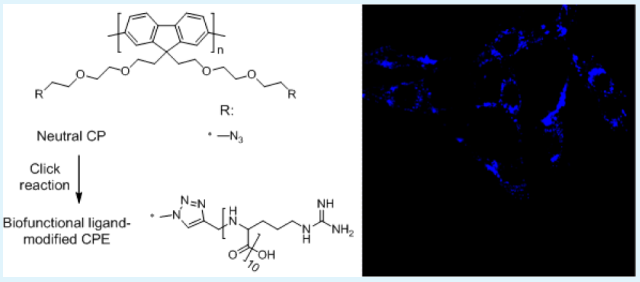

KEYWORDS: *polyfluorene, conjugated polyelectrolyte, oligopeptide, click reaction, cellular imaging*

Conjugated polyelectrolytes (CPEs) are water-soluble macromolecules characterized with delocalized conjugated backbones and ionic side chains.[1] They inherit the general optoelectronic properties from their neutral counterparts (organic soluble conjugated polymers) and charged functionalities from polyelectrolytes, which make them a unique category of functional materials in optoelectronic devices and biosensor applications.[2−5] Recently, CPEs have been applied in cellular imaging,[6−11] extracellular matrix protein imaging,[12] intracellular protein imaging[13] and in vivo drug tracking,[14] as they can ideally fulfill the criteria of a good fluorescent probe, such as good water solubility, high brightness, excellent photostability and low cytotoxicity.

Advances in the development of chemistry and material science boomed the preparation of CPEs *via* conjugated backbone or side chain modification.[15] Generally, synthesis of CPEs is accessible either by postionization of preprepared polymers[16−19] or directly by polymerization between ionic monomers.[20−22] Both strategies have their merits and limitations. For postionization method, the monomers and precursor polymers are soluble in common organic solvents, which can be easily purified by well-known techniques employed in organic polymer chemistry, but the final CPEs may possess ion distribution defects on their side chains due to incomplete ionization. On the other hand, direct polymerization between ionic monomers enables the final CPEs with perfect ions distribution on side chains, but it is difficult to purify their monomers and the final CPE products.

To obtain CPEs for special biological applications, such as protein detection[23] and targeted cellular imaging,[16,18,24,25] biofunctional ligands (e.g., peptide, antibody, protein) were attached to the side chains of CPEs via pre- or postfunctionalization. Biofunctional ligands generally possess high polarity, which often leads to difficulties in purification. For example, Müllen et al. reported poly(2,7-carbozole)-based CPE with poly($_L$-lysine) as side chains via a macromonomer approach.[26] The synthetic route undergoes tedious protection/deprotection steps, and the steric hindrance of macromonomers makes it very difficult to control the polymerization processes. The crucial steps for postfunctionalization method involved in the preparation of CPEs with special biofunctional ligands include (i) the synthesis of CPEs with functional groups (such as free NH_2, COOH) for further conjugation, and (ii) postconjugation chemistry between CPEs and biofunctional ligands. These synthetic steps often suffer from tedious synthetic procedures, low yield and harsh purification problems. Moreover, the electrostatic interactions between the precursor CPEs and biofunctional ligands contribute more obstacles to purify the final products.

In this contribution, we report a facile strategy to prepare CPE with biofunctional ligands through efficient click reaction. An oligoarginine (RRRRRRRRRR) (R10) is directly attached onto the side chains of a neutral polyfluorene to yield PF-R10 as a model CPE to demonstrate our synthetic strategy. Click reaction is selected as the key step for the CPE synthesis,

Special Issue: Forum on Conjugated Polymer Materials for Sensing and Biomedical Applications

Received: January 14, 2013
Accepted: February 28, 2013
Published: February 28, 2013

   dx.doi.org/10.1021/am400169v | *ACS Appl. Mater. Interfaces* 2013, 5, 4511−4515

Scheme 1. Synthetic Route towards PF-R10[a]

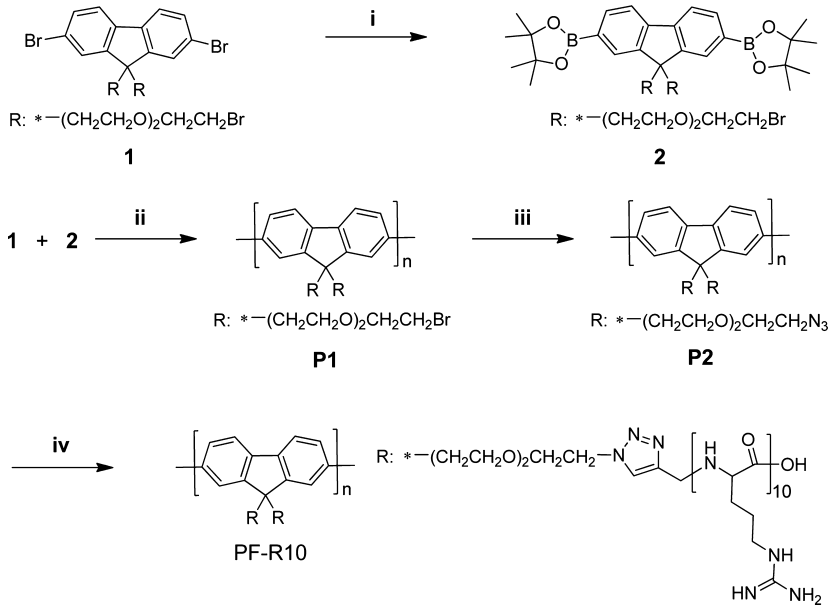

[a]Reagents and conditions: (i) $Pd(dppf)_2Cl_2$, AcOK, bis(pinacolato)diboron, anhydrous dioxane, 85 °C, 15 h; (ii) $Pd(PPh_3)_4$, Et_4NOH, toluene, 85 °C, 24 h; (iii) THF/DMSO, NaN_3, 70 °C, 2 days; (iv) THF/DMSO, $CuSO_4$, sodium ascorbate, room temperature.

because it is a versatile coupling strategy with high reaction yield and broad tolerance toward various solvents and functional groups.[27,28] The obtained PF-R10 is characterized, and its pH-dependent optical properties are discussed. Further cellular imaging studies reveal the excellent cell penetration and labeling ability of PF-R10 for fluorescence imaging.

Scheme 1 shows the synthetic route toward PF-R10. 9,9-Bis(2-(2-(2-bromoethoxy)ethoxy)ethyl)-2,7-bis(4,4,5,5-tetramethyl-1,3,2-dioxaborolan-2-yl)fluorene **2** was synthesized in 59% yield by Suzuki-Miyauri reaction from 2,7-dibromo-9,9-bis(2-(2-(2-bromoethoxy)ethoxy)ethyl)fluorene **1** in the presence of bis(pinacolato)diboron, CH_3COOK and $Pd(dppf)_2Cl_2$ in anhydrous dioxane at 85 °C for 15 h. Suzuki polymerization between **1** and **2** in toluene at 85 °C for 20 h yielded poly[9,9-bis(2-(2-(2-bromoethoxy)ethoxy)ethyl)fluorene-2,7-diyl] **P1** in 67% yield, using $Pd(PPh_3)_4$ and Et_4NOH as the catalyst system. After treatment with NaN_3 in THF/DMSO at 70 °C for 2 days, **P1** was successfully converted into poly[9,9-bis(2-(2-(2-azidoethoxy)ethoxy)ethyl)fluorene-2,7-diyl] **P2** in 92% yield. The number-average molecular weight (M_n) and polydispersity index (PDI) evaluated by gel permeation chromatography (GPC) are 9800 (2.1) for **P1** and 8500 (1.9) for **P2**, respectively. During the purification of **P2**, small molecular weight fractions of **P2** were removed by precipitation. On the other hand, some of the polymer fraction with large molecular weight was also removed by filtration. Both factors contribute to the relatively narrower PDI and smaller molecular weight of **P2** with respect to those of **P1**. As **P2** possesses azido groups at the end of side chains, click chemistry with an oligopeptide propargyl-RRRRRRRRRR was performed in the presence of $CuSO_4$/sodium ascorbate in THF/DMSO mixture to afford PF-R10, which was purified by dialysis against water followed by running through a PD-10 column to remove catalyst and free peptide. The final product of PF-R10 was kept in aqueous solution in refrigerator at 4 °C as the stock solution for further use.

The chemical structure of the intermediates was confirmed by NMR spectra. The singlet at 1.39 ppm for **2** is attributed to the methyl protons from 4,4,5,5-tetramethyl-2,1,3-dioxaborolane-2-yl group, and the integrated area ratio between the peaks at 1.39 ppm and 3.66 ppm (OCH_2CH_2Br) is calculated to be 6, which indicates the correct structure of **2**. When compared to the ^1H NMR spectra of **1** and **2**, the broadened signals for **P1** are indicative of the success of the polymerization. As compared to **P1**, the signal at 3.66 ppm (OCH_2CH_2Br) reduces sharply accompanied by the appearance of a new peak at 3.54 ppm ($OCH_2CH_2N_3$), suggesting the successful conversion of bromo to azido group. The conversion yield was calculated to be ~89% based on the integrated area ratio between the peaks at 3.66 and 3.54 ppm. The number of N_3 group was calculated to be ~31 on average for each polymer chains. As the molecular weight of PF-R10 is not easily determined by gel permeation chromatography (GPC) due to its ionic characteristic and large brushed side chains, the molecular weight of PF-R10 was calculated to be 58600 based on the M_n of precursor polymer **P2** and the peptide-graft efficiency.

The change of functional groups from **P1** to **P2** and PF-R10 was also monitored by FTIR spectra. As shown in Figure 1, the appearance of a strong peak for **P2** at 2094 cm^{-1} corresponding to the stretching vibration band of N_3 with respect to that for **P1** demonstrates the successful conversion of Br to N_3, which is consistent with the ^1H NMR results. After click reaction, no signals are observed around 2100 cm^{-1} (corresponding to the stretching vibration bands of N_3 and C≡C) for PF-R10, which indicates that nearly all the N_3 groups have been consumed in PF-R10.

Figure 2A shows the normalized UV−vis and PL spectra of PF-R10 in water. PF-R10 has an absorption peak at ~380 nm, due to $\pi-\pi^*$ transition of the conjugated backbone. PF-R10 shows well-defined vibronic transitions characterized with a peak at 430 nm and two shoulders at 447 and 470 nm, which are consistent with previously reported polyfluorenes.[29] The quantum yield (QY) of PF-R10 in water was calculated to be

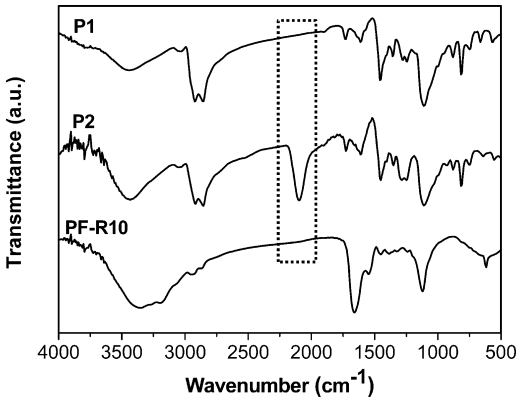

Figure 1. FTIR spectra of **P1**, **P2**, and PF-R10.

7% using quinine sulfate in 0.1 M H_2SO_4 aqueous (QY = 54%) as the standard.[30]

As PF-R10 possesses both amine and carboxylic acid groups, the pH change of aqueous media may influence the polymer charge density, and in turn its fluorescent property. As such, we investigated the fluorescence property of PF-R10 in the absence and presence of HCl. Figure 2B shows the PL spectra of 4.5 μM PF-R10 upon varying HCl concentrations from 0 to 24 μM at intervals of 2 μM. A significant enhancement in the fluorescence intensity is clearly observed with increasing HCl concentrations and the saturation occurs at [HCl] $\approx$ 20 μM. This is also accompanied by a blue-shift in emission maximum from 430 to 424 nm. The dramatic increase in fluorescence intensity can be attributed to the protonation of PF-R10 side chains and the electrostatic repulsion reduce aggregation of polymer backbone which can cause fluorescence quenching.[31] The blue-shifted emission is due to the reduced aggregation. By contrast, only slight fluorescence enhancement was observed for PF-R10 upon addition of NaOH (see Figure S1 in the Supporting Information) because of the conversion from carboxylic acid to carboxylate which slightly improves the hydrophilicity of the polymer.[32] It is worth noting that the fluorescence difference between PF-R10 in acidic and basic conditions is due to the different numbers of amine and carboxylic acid groups presented on R10. Considering that the fluorescence characteristic of PF-R10 is strongly pH-dependent, it has the potential to be used as a pH probe.

To verify the hypothesis that the fluorescence enhancement for PF-R10 in acidic condition is indeed due to the reduced aggregation, we studied the self-assembly behaviors of pristine PF-R10 and protonated PF-R10 in water by laser light scattering (LLS). According to the amphiphilic chemical structure of PF-R10, it is expected that the hydrophobic conjugated backbones are likely to be embedded inside, while the hydrophilic peptide side chains are likely to be extended outside in aqueous media. As shown in Figure 3A, PF-R10

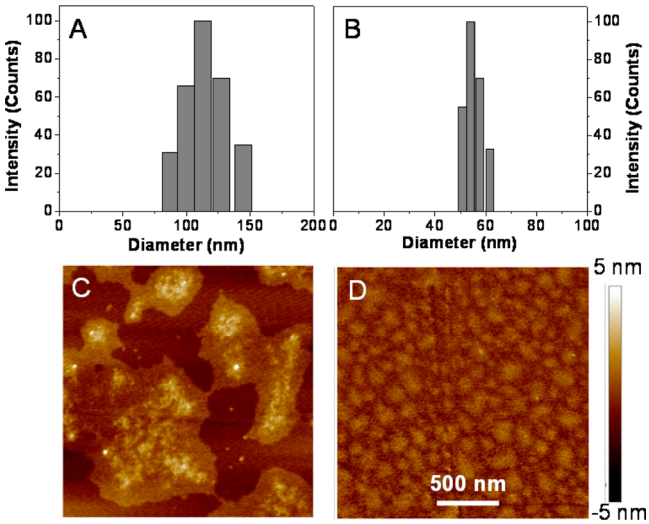

Figure 3. Hydrodynamic diameter of (A) pristine PF-R10 and (B) protonated PF-R10 in water with [PF-R10] = 4.5 μM. Tapping-mode AFM height images (scan size 2 × 2 μm) of spin-coated (C) pristine PF-R10 and (D) protonated PF-R10 from Milli-Q water. [HCl] = 24 μM for the protonated PF-R10 in B and D. C and D share the same scale bar.

shows a mean hydrodynamic diameter of 112 nm, by contrast, the protonated PF-R10 exhibits a reduced hydrodiameter of 54 nm with a relatively narrow size distribution (Figure 3B), which clearly indicates the less aggregated state of protonated PF-R10 in water as compared to that of pristine PF-R10. The LLS results also suggest that both the pristine and protonated PF-R10 are dispersed in water as nanoparticles. In addition, the surface morphologies of pristine PF-R10 and protonated PF-R10 were also evaluated by atomic force microscopy (AFM). The solutions of pristine PF-R10 and protonated PF-R10 were spin-coated on mica for AFM measurements, and their respective AFM images are shown in images C and D in Figure 3. The pristine PF-R10 shows severe aggregation with a height of 2−5 nm, while the protonated PF-R10 shows less aggregated state with a height of 0.5−2 nm. Both LLS and AFM results consistently support that the fluorescence increase is indeed derived from the reduced aggregation state of PF-R10 from neutral to acidic conditions.

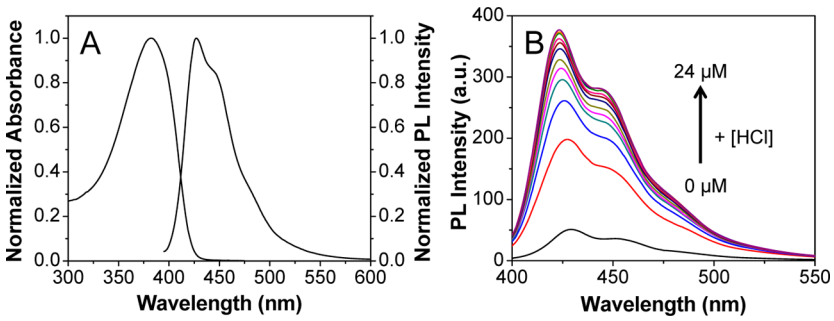

Figure 2. (A) Normalized UV−vis and PL spectra of PF-R10 in water. (B) PL spectra of PF-R10 with [HCl] ranging from 0 to 24 μM at intervals of 2 μM. [PF-R10] = 4.5 μM based on repeat unit. Excitation at 380 nm.

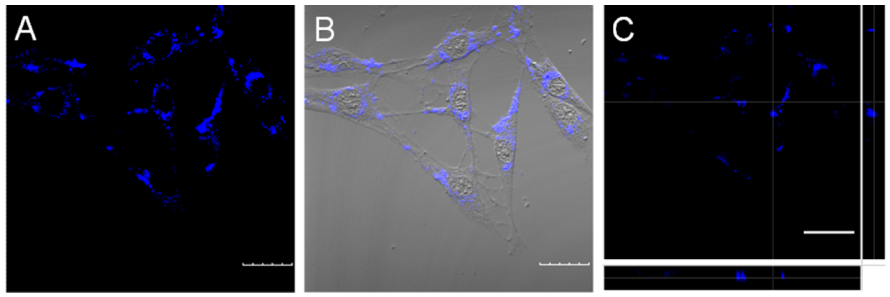

Figure 4. (A) CLSM fluorescence, (B) fluorescence/transmission overlay, and (C) 3D images of MCF-7 breast cancer cells after incubation with 5 μM PF-R10 at 37 °C overnight. The scale bar is 30 μm.

To demonstrate the applicability of PF-R10 as a fluorescent probe for in vitro cellular imaging, MCF-7 breast cancer cells were used as a model to visualize its cell uptake and imaging. After incubation with 5 μM PF-R10 based on repeat unit at 37 °C overnight, the cells were fixed and imaged by the confocal laser scanning microscopy (CLSM). The confocal images were taken upon excitation at 405 nm with a power of 1.25 mW, and the fluorescence signals were collected from 430 to 470 nm. When compared to the image of blank MCF-7 cancer cells (not shown), bright blue fluorescence was observed throughout the cell cytoplasm as shown in Figure 4A. The boundary between cell nucleus and cytoplasm can be clearly distinguished, indicating an efficient uptake of PF-R10 by MCF-7 cells. In addition, the merged fluorescence/transmission image of MCF-7 cells displayed in Figure 4B suggests that the PF-R10 is mainly located in the cytoplasm, which is further confirmed by the corresponding 3D CLSM image (Figure 4C). As no fluorescence can be detected from the blank cells under the same experimental setup, it is confirmed that the fluorescence from the cells in Figure 4A is indeed derived from PF-R10 rather than autofluorescence, which further reveals that PF-R10 can be efficiently internalized by MCF-7 cells and accumulated in the cytoplasm. The efficient uptake of PF-R10 by MCF-7 cells can be attributed to the cell-penetrating property of the grafted R10 oligopeptide.[33]

The cytotoxicity of PF-R10 against MCF-7 cells was evaluated by methylthiazolyldiphenyl-tetrazolium (MTT) cell viability assays. Figure 5 shows the in vitro MCF-7 cells viability after incubation with the PF-R10 at the concentrations of 5, 50, and 100 μM for 24 and 48 h, respectively. The cell viabilities are close to 100% within the tested period of time, indicating low cytotoxicity of PF-R10 toward MCF-7 cells under the experimental conditions. Noteworthy is that the cell viabilities are still higher than 90% even at 100 μM, a concentration that is 20-fold higher of that used for imaging. The low cytotoxicity of PF-R10 makes it safe for long-term cellular imaging and other clinical applications.

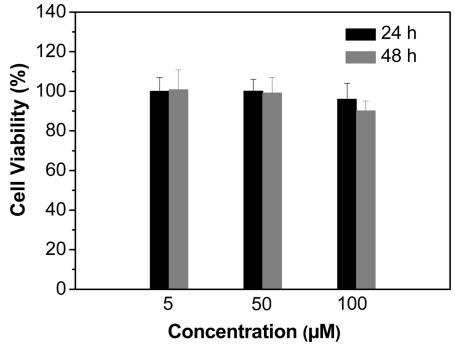

Figure 5. Metabolic viability of MCF-7 cancer cells after incubation with PF-R10 at concentrations of 5, 50, and 100 μM for 24 and 48 h, respectively.

In conclusion, we report a facile yet effective strategy to synthesize CPEs with oligopeptide as the side chains. Amphiphilic oligopeptide was directly incorporated on neutral azido-modified conjugated polymers via click chemistry to afford PF-R10. The presented strategy toward biologically functionalized CPEs through directly biofunctionalization of neutral conjugated polymer significantly eliminates the tedious synthesis and purification procedures. The representative CPE, PF-R10 shows significant fluorescence enhancement in acidic environment as compared to that in water, due to the protonated amine groups and electrostatic repulsion which reduce the aggregation-induced fluorescence quenching. Fluorescence cellular imaging by CLSM using MCF-7 cancer cells as a model cell line successfully demonstrated the capability of PF-R10 as a fluorescent probe with low cytotoxicity and high fluorescence contrast. The demonstrated strategy herein not only facilitates the synthetic procedures of ligand-modified CPEs but also encourages future simple design of near-infrared fluorescent CPEs for specific targeted bioimaging.

■ ASSOCIATED CONTENT

Supporting Information

Experimental section including materials, instrumentation, synthesis, cell culture, cellular imaging, cytotoxicity assays, and the PL spectra of PF-R10 upon varying NaOH concentration. This material is available free of charge via the Internet at http://pubs.acs.org/.

■ AUTHOR INFORMATION

Corresponding Author

*E-mail: cheliub@nus.edu.sg. Tel.: 65-6516-8049. Fax: (+65) 6779-1936.

Notes

The authors declare no competing financial interest.

■ ACKNOWLEDGMENTS

The authors are grateful to Temasek Defence Systems Institute (ARF R-279-000-305-592/422/232) and Singapore Ministry of Defense (R279-000-340-232) for financial support.

■ REFERENCES

(1) Pinto, M. R.; Schanze, K. S. *Synthesis* **2002**, 1293−1309.

(2) Huang, F.; Hou, L.; Wu, H.; Wang, X.; Shen, H.; Chao, W.; Yang, W.; Cao, Y. *J. Am. Chem. Soc.* **2004**, *126*, 9845−9853.
(3) Seo, J. H.; Gutacker, A.; Walker, B.; Cho, S.; Garcia, A.; Yang, R.; Nguyen, T. −Q.; Bazan, G. C. *J. Am. Chem. Soc.* **2009**, *131*, 18220−18221.
(4) Thomas, S. W., III; Joly, G. D.; Swager, T. M. *Chem. Rev.* **2007**, *107*, 1339−1386.
(5) Feng, X.; Liu, L.; Wang, S.; Zhu, D. *Chem. Soc. Rev.* **2010**, *39*, 2411−2419.
(6) Pu, K.; Liu, B. *Adv. Funct. Mater.* **2011**, *21*, 3408−3423.
(7) Zhu, C.; Liu, L.; Yang, Q.; Lv, F.; Wang, S. *Chem. Rev.* **2012**, *112*, 4687−4735.
(8) Kim, I. B.; Shin, H.; Garcia, A. J.; Bunz, U. H. F. *Bioconjugate Chem.* **2007**, *18*, 815−820.
(9) Pu, K.; Li, K.; Shi, J.; Liu, B. *Chem. Mater.* **2009**, *21*, 3816−3822.
(10) Pu, K.; Li, K.; Liu, B. *Adv. Funct. Mater.* **2010**, *20*, 2770−2777.
(11) Pu, K.; Li, K.; Liu, B. *Chem. Mater.* **2010**, *22*, 6736−6741.
(12) McRae, R. L.; Phillips, R. L.; Kim, I. B.; Bunz, U. H. F.; Fahrni, C. J. *J. Am. Chem. Soc.* **2008**, *130*, 7851−7853.
(13) Li, K.; Pu, K.; Cai, L.; Liu, B. *Chem. Mater.* **2011**, *23*, 2113−2119.
(14) Ding, D.; Li, K.; Zhu, Z.; Pu, K.; Hu, Y.; Jiang, X.; Liu, B. *Nanoscale* **2011**, *3*, 1997−2002.
(15) Pu, K. Y.; Wang, G.; Liu, B. In *Conjugated Polyelectrolytes: Fundamentals and Applications*; Liu, B., Bazan, G. C., Eds.; Wiley-VCH: Germany, 2013; pp 1−64.
(16) Chaturvedi, V.; Tanaka, S.; Kaeriyama, K. *Macromolecules* **1993**, *26*, 2607−2611.
(17) Brodowski, G.; Horvath, A.; Ballauff, M.; Rehahn, M. *Macromolecules* **1996**, *29*, 6962−6965.
(18) Balanda, P. B.; Ramey, M. B.; Reynolds, J. R. *Macromolecules* **1999**, *32*, 3970−3978.
(19) Jiang, H.; Taranekar, P.; Reynolds, J. R.; Schanze, K. S. *Angew. Chem., Int. Ed.* **2009**, *48*, 4300−4316.
(20) Child, A. D.; Reynolds, J. R. *Macromolecules* **1994**, *27*, 1975−1977.
(21) Faïd, K.; Leclerc, M. *Chem. Commun.* **1996**, 2761−2762.
(22) Burrows, H. D.; Lobo, V. M. M.; Pina, J.; Ramos, M. L.; Seixas de Melo, J.; Valente, A. J. M.; Tapia, M. J.; Pradhan, S.; Scherf, U. *Macromolecules* **2004**, *37*, 7425−7427.
(23) Phillips, R. L.; Kim, I. -B.; Tolbert, L. M.; Bunz, U. H. F. *J. Am. Chem. Soc.* **2008**, *130*, 6952−6954.
(24) Liu, J.; Ding, D.; Geng, J.; Liu, B. *Polym. Chem.* **2012**, *3*, 1567−1575.
(25) Pu, K.; Shi, J.; Cai, L.; Li, K.; Liu, B. *Biomacromolecules* **2011**, *12*, 2966−2974.
(26) Fruth, A.; Klapper; Markus, M.; Müllen, K. *Macromolecules* **2010**, *43*, 467−472.
(27) Kolb, H. C.; Finn, M. G.; Sharpless, K. B. *Angew. Chem., Int. Ed.* **2001**, *40*, 2004−2021.
(28) Stanley, L. M.; Sibi, M. P. *Chem. Rev.* **2008**, *108*, 2887−2902.
(29) Wang, H.; Lu, P.; Wang, B.; Qiu, S.; Liu, M.; Hanif, M.; Cheng, G.; Liu, S.; Ma, Y. *Macromol. Rapid Commun.* **2007**, *28*, 1645−1650.
(30) Demas, J. N.; Crosby, G. A. *J. Phys. Chem.* **1971**, *75*, 991−1024.
(31) Lee, S. H.; Kömürlü, S.; Zhao, X.; Jiang, H.; Moriena, G.; Kleiman, V. D.; Schanze, K. S. *Macromolecules* **2011**, *44*, 4742−4751.
(32) Qin, C.; Wu, X.; Tong, H.; Wang, L. *J. Mater. Chem.* **2010**, *20*, 7957−7964.
(33) Futaki, S.; Suzuki, T.; Ohashi, W.; Yagami, T.; Tanaka, S.; Ueda, K.; Sugiura, Y. *J. Biol. Chem.* **2001**, *276*, 5836−5840.